Engineering Geology 187 (2015) 122–134

Contents lists available at ScienceDirect

Engineering Geology

journal homepage: www.elsevier.com/locate/enggeo

Technical Note

Statistical and probabilistic analyses of impact pressure and discharge of debris flow from 139 events during 1961 and 2000 at Jiangjia Ravine, China

Y. Hong [a], J.P. Wang [b], D.Q. Li [c], Z.J. Cao [c,*], C.W.W. Ng [b], P. Cui [d]

[a] College of Civil Engineering and Architecture, Zhejiang University, Hangzhou, China
[b] Department of Civil and Environmental Engineering, Hong Kong University of Science and Technology, Kowloon, HKSAR, China
[c] State Key Laboratory of Water Resources and Hydropower Engineering Science, School of Water Resources and Hydropower Engineering, Wuhan University, Wuhan, China
[d] Key Laboratory of Mountain Hazards and Earth Surface Process, Institute of Mountain, Hazards and Environment, Chinese Academy of Sciences, Chengdu, China

ARTICLE INFO

Article history:
Received 5 September 2014
Received in revised form 30 November 2014
Accepted 26 December 2014
Available online 30 December 2014

Keywords:
Statistical and probabilistic analyses
Gaussian copula approach
Debris flow
Field data
Impact pressure
Discharge

ABSTRACT

Debris flows often cause catastrophic damage to communities in the downstream area, by direct impact and deposition. Theoretical predictions of impact pressure and volume of discharge, however, still remain very challenging, mainly due to inadequate understanding of the complex problems and limited field data at the local scale. In this study, the maximum impact pressure (P_{max}) and total discharge (Q_{total}) of 139 debris flow events that occurred during 1961 and 2000 in the "debris museum" of China (i.e., the Jiangjia Ravine) are reported and interpreted with statistical tests and probabilistic analyses. Four common probabilistic models (Normal, Lognormal, Weibull and Gamma distributions) are used to simulate the distributions of P_{max} and Q_{total}. The level of fitting of each model is assessed by performing two quantity-based statistic goodness-of-fit tests (Chi-square and Kolmogorov–Smirnov tests). The field data show that during the period from 1961 to 2000, the maximum values of P_{max} and Q_{total} are 744 kPa and 1,751,537 m^3, respectively. It is suggested by the goodness-of-fit tests that the Weibull distribution is the only model (among the four probabilistic models) that is able to capture the distributions of P_{max} and Q_{total} of both surge and continuous flows. Using the verified Weibull distributions and Gaussian copula approach, univariate and bivariate exceedance probability charts considering P_{max} and Q_{total} are developed. Regression models between P_{max} and Q_{total} are also established.

© 2014 Elsevier B.V. All rights reserved.

1. Introduction

Catastrophic hazards due to debris flow are frequently encountered in mountainous areas all over the world. Debris flow imposes destructive threats to infrastructures (transportation systems, buildings and lifelines) and inhabitants in the downstream areas, by direct impact and sediment deposition (Ngadisih et al., 2014). China is a country in which debris flows are frequently encountered. According to Kang et al. (2004), approximately 45% of the area of China (10^6 km^2) has suffered from debris flows. For example, the recent destructive hazard that occurred in Southern China (Zhouqu, in Gansu Province) in 2010 claimed 1467 lives and buried two villages. Despite the hazardous consequences of debris flows, many infrastructures still need to be constructed in mountainous areas, due to scarcity of usable land.

In order to protect the infrastructures and people from debris flows, one common solution is to construct either rigid or flexible barriers above the downstream area. Rational design of any barrier system largely depends on reasonable estimations of the maximum impact pressure (P_{max}) and total discharge (Q_{total}) induced by a debris flow. In addition to their importance in engineering design, P_{max} and Q_{total} are also two key elements to gauge the risk of the debris flow. Currently, it is still challenging to predict P_{max} and Q_{total} (Iverson, 1997; Eidsvig et al., 2014; Gartner et al., 2014), due to limited understanding of the complex behaviour of debris flows (Chang et al., 2011; Hu et al., 2011). In addition, there is a lack of field data of P_{max} and Q_{total} at the local scale (Liang et al., 2012).

As a result, the key scope of this study is to present and analyse the statistics of P_{max} and Q_{total} from 139 debris flow events that occurred in the Jiangjia Ravine, China. Statistical analyses on the field data are carried out by simulating the distributions of P_{max} and Q_{total} using four common probabilistic models (Normal, Lognormal, Weibull and Gamma distributions). The level of fitting of each model is assessed by performing two statistical goodness-of-fit tests (Chi-square and Kolmogorov–Smirnov tests). Probabilistic models which are not rejected by the goodness-of-fit tests are then used to develop exceedance probability charts, for the estimation of P_{max} and Q_{total}. Not only does this study aim at developing site-specific semi-empirical equations and design charts for local authorities, but it is also intended to shed light on the natural variability of debris flow from a statistical perspective.

* Corresponding author.
E-mail address: zijuncao@whu.edu.cn (Z.J. Cao).

http://dx.doi.org/10.1016/j.enggeo.2014.12.011
0013-7952/© 2014 Elsevier B.V. All rights reserved.

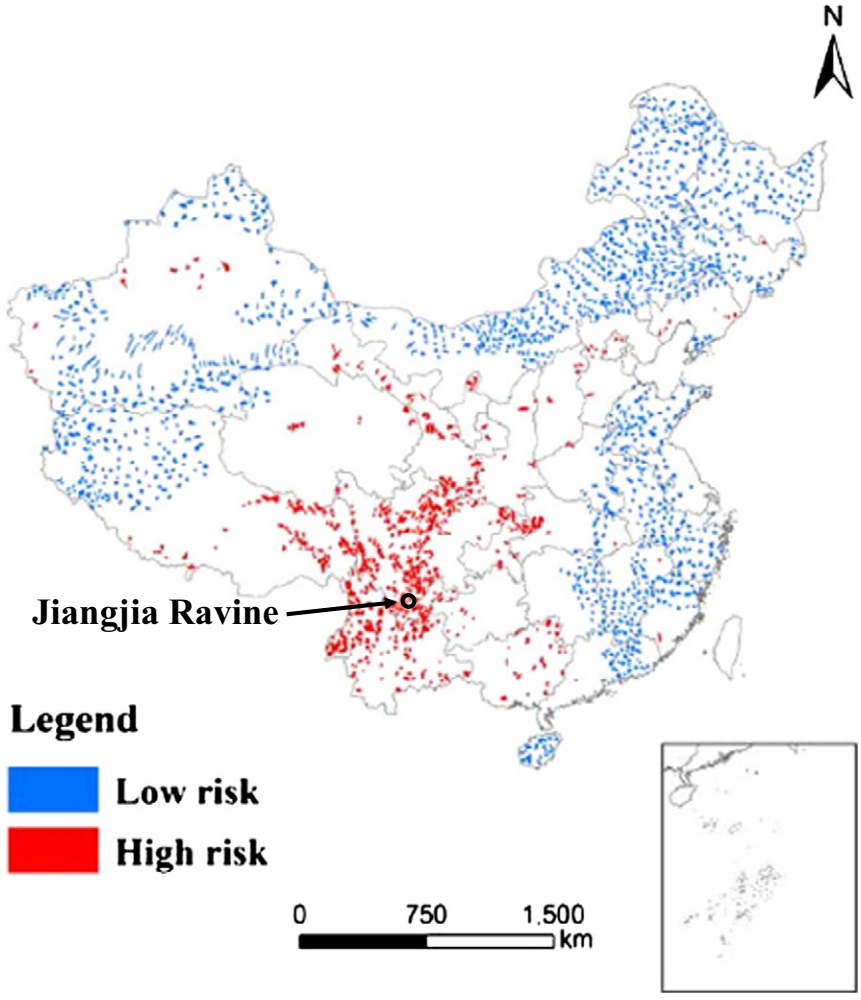

(a)

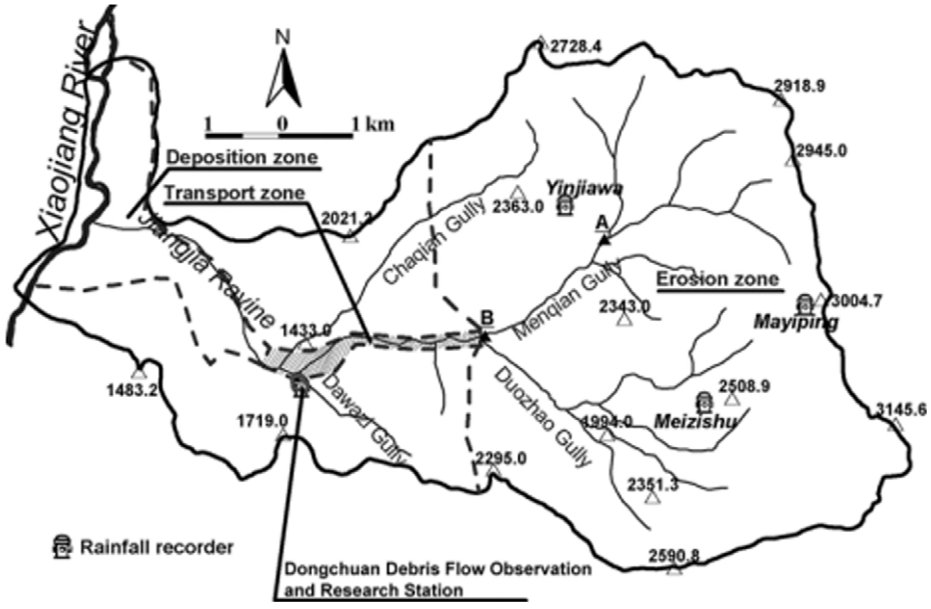

Note: each number denotes elevation above sea level (unit: m)

(b)

Fig. 1. (a) Spatial distribution of debris flow hazards in China (modified from Liang et al., 2012); (b) Plan view of Jiangjia Ravine (Cui et al., 2005).

2. Field measurement in Jiangjia Ravine, China

2.1. Study area

Debris flows in China are very active in the southwestern mountainous regions, particularly in the Dongchuan area of Yunan Province. Within the Dongchuan area, debris flows in the Jiangjia Ravine are infamous for their high frequency of occurrence (up to 28 times per year) and great damage to local infrastructures. Accordingly, the ravine is widely regarded as the "debris museum" in China. Fig. 1(a) shows the location of the study area (i.e., Jiangjia Ravine in Yunan Province), which is classified as one of the few high risk regions suffering from debris flows (Liang et al., 2012). As shown in Fig. 1(b), the Jiangjia Ravine, which has an area of 48.6 km^2, is positioned in the Xiaojiang fault, which is characterised as intense tectonism (Cui et al., 2005).

Debris flows in this region mostly occur during rainy seasons (from June to September), with more than 80% of the annual rainfall (ranging from 700 to 1200 mm) in this period (Hu et al., 2011). Triggered by the heavy rainfalls, the exposed materials (i.e., highly fractured rocks, weak sandstone and slate, colluvium and mantle rock) in the Jiangjia Ravine were eroded and mixed as clastic detritus, forming the main source of the debris flow (Zhou and Ng, 2010). Fig. 2 shows the typical particle size distributions of the debris flow in the study area (Cui et al., 2005; Kang et al., 2006). Previous field studies showed that the bulk density of the debris flows was in the range from 1600 to 2300 kg/m^3, and that the volumetric solid fraction was up to 85% (Li and Yuan, 1983; Zhang, 1993; Cui et al., 2005).

2.2. Monitoring station and data collection

In view of the uniqueness of the Jiangjia Ravine, a permanent monitoring station (i.e., Dongchuan Debris Flow Observation and Research Station, or DDFORS) was set up near the downstream area of the ravine (N26°14′, E103°08′) in the early 1960s, by the Institute of Mountain Hazards and Environment Chinese Academy of Science (Cui et al., 2005). This is the only semi-automatic field observation station investigating debris flow in China (Zhou and Ng, 2010).

The monitoring programme of the station records the channel width (W), thickness of debris flow (h), density (ρ) of each surge, duration (t) of each surge and front velocity (v). The first two parameters (W and h) were directly measured at the site, while ρ was obtained by laboratory tests on samples taken from each debris flow. To obtain t and v of a debris flow, two monitoring sections along a straight channel were selected. With a known distance (L) between the two monitoring sections and the measured duration t (by a stopwatch) for the surge front to pass through L, the mean front velocity v can be calculated (i.e., $v = L / t$).

Based on the measurements, two key parameters of a debris flow, i.e., impact pressure (P) and volume of discharge (Q), can be determined as $P = \rho v^2$ (according to hydrodynamics) and $Q = LWh$. All field data of debris flows in the Jiangjia Ravine from 1961 to 2000 are summarised and reported in three documents by Zhang and Xiong (1997), Kang et al. (2006, 2007). During the forty years, there have been about 247 debris flow events, 56% (i.e., 139 events) of which were recorded by the monitoring station and presented in the three documents. According to the field data, each flow usually consists of dozens of surge flows and a few continuous flows. A surge flow is defined as a flow having obvious breaks between two continual surges, or flows with relatively short duration, while a continuous flow refers to a flow lasting for a relatively long duration and producing a large amount of discharge (Zhang and Xiong, 1997; Kang et al., 2006, 2007). For each debris flow event, only the maximum value of impact pressure (P_{max}) and the total amount of the discharge (Q_{total}) of the surge and continuous flows are presented in this study, to represent the worst case scenario. To be more specific, the database reported in this study includes a total number of 278 data points for surge flows (139 data for both Q_{total} and P_{max}) and 236 for continuous flows (118 data for both Q_{total} and P_{max}). All the measured data for surge and continuous flows are summarised in Tables A.1 and A.2, respectively (see Appendix A).

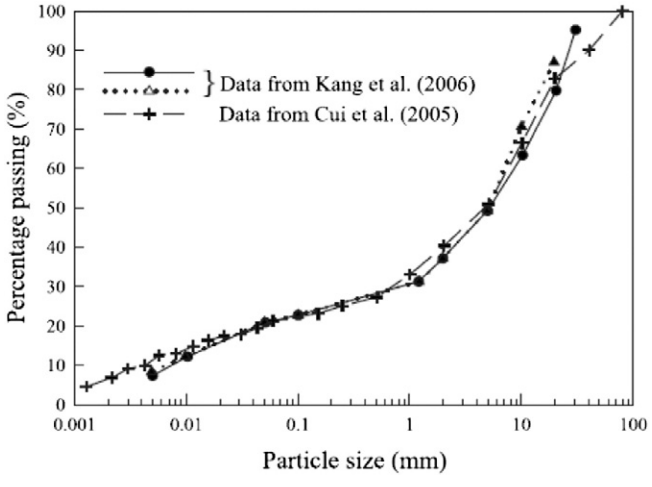

Fig. 2. Particle-size distribution of the natural debris flows at the Dongchuan Debris flow Observation and Research Station, China (Zhou and Ng, 2010).

3. Statistical analysis

3.1. Probability models

To analyse the observed distribution of the maximum impact pressures (P_{max}) and total discharges (Q_{total}) under a probabilistic framework, four commonly used probability models (i.e., Normal, Lognormal, Gamma and Weibull distributions) are adopted in this study. It is worth noting that before the probabilistic simulation, there was no prior knowledge regarding the suitability of each model for predicting the distributions of P_{max} and Q_{total}. The parameters for each model were converted from the statistics (i.e., mean and standard deviation) of P_{max} and Q_{total} based on the 139 debris flow events in the Jiangjia Ravine.

3.2. Statistical goodness-of-fit tests

To quantitatively access whether the four models can satisfactorily simulate the distributions of P_{max} and Q_{total} in the Jiangjia Ravine, two quantity-based statistical goodness-of-fit tests (i.e., Chi-square and Kolmogorov–Smirnov tests) are carried out. In the Chi-square goodness-of-fit test, the measured data are sorted into k-intervals. Subsequently, the difference between the measured frequencies (n_i) and the theoretical frequencies (e_i) by a selected probability model was quantified by calculating χ^2 ($\sum_{i-1}^{k} \frac{(n_i - e_i)^2}{e_i}$), which should approach the Chi-square distribution (Ang and Tang, 2007; Fenton and Griffiths, 2008). Once the calculated χ^2 is less than a critical value following the Chi-square distribution at a given level of significance (usually 5% in the statistical test), the selected probability model may be suitable to model the variables (i.e., P_{max} and Q_{total} in this study) examined, and vice versa. It is well recognised that subjectivity is involved in the Chi-square test for selecting a bin size of the histograms, although the influence of the bin size is usually insignificant (Wang et al., 2011, 2014). The Kolmogorov–Smirnov test, in which the subjectivity in determining bin size is eliminated, is therefore also performed in this study. In a Kolmogorov–Smirnov test, the maximum differences

(D_n) between the observed and the theoretical cumulative probabilities over the entire range are calculated and compared to a critical value, which can be readily determined based on the samples size and the level of significance used. Any selected model with a D_n less than the critical value is considered as acceptable for the simulation, and vice versa. In this study, a level of significance of 5% was adopted in both Chi-square and Kolmogorov–Smirnov tests.

The aforementioned probability analyses and statistical goodness-of-fit tests are performed with an Excel Spreadsheet, which is developed in-house.

4. Interpretation of the measured results

4.1. Statistics of the maximum impact pressure and total discharge

Based on the collected data (i.e., P_{max} and Q_{total}) of the surge and continuous flows from the 139 events, statistics such as mean, standard deviations (SD) and coefficient of variation (COV) can be derived (Ang and Tang, 2007; Wang and Cao, 2013; Jiang et al., 2014a, b; Li et al., 2014). With the mean and SD, the parameters of the four selected probabilistic models can be calculated. Table 1 summarises the statistics of P_{max} and Q_{total} of the 139 debris flow events, as well as the model parameters calculated with the statistics. It is worth noting that both method of moments (MM) and maximum likelihood method (MLM) were attempted to estimate the distributions parameters of P_{max} and Q_{total}. Similar distributions were resulted, based on the distribution parameters obtained from MM and MLM. Considering MM is relatively simple and intuitive as compared with MLM (Fenton and Griffiths, 2008), all distribution parameters in this study (see Table 1) are calculated based on MM.

It can be seen that the COVs of $P_{\max}$ of the surge and continuous flows are 0.5 and 0.8, respectively. Comparatively, the data of Q_{total} show a much larger variation, with COV equal to 1.0 and 1.7 for the surge and continuous flows, respectively. This is probably because $P_{\max}$ is obtained from one single flow. While each Q_{total} is the sum of discharge of either surge flows or continuous flows in each debris flow event. Thus, the former is likely to involve less uncertainty (which results in smaller COV) than the latter. As far as flow type is concerned, Q_{total} and $P_{\max}$ of the continuous flow exhibit larger natural variability (as indicated by COV) than those of the surge flow. Comparisons between the two types of flows also show that larger $P_{\max}$ (maximised at 744 kPa) is induced by surge flows, as compared with that (maximised at 434 kPa) caused by the continuous flows. Although the mean value of Q_{total} for the surge flow (240,447 m^3) is larger than that for the continuous flow (161,169 m^3), the maximum value of Q_{total} for the surge flow (1,260,549 m^3) is smaller than that for the continuous flow (1,751,537 m^3).

Table 1
Statistics of the maximum impact pressure and total discharge from 1960 to 2000 in Jiangjia Ravine, China.

Parameter	Value			
	Maximum impact pressure $P_{\max}$ (kPa)		Total discharge Q_{Total} (m^3)	
	Surge flow	Continuous flow	Surge flow	Continuous flow
Mean	221	114	240,447	161,169
Standard deviation (SD)	102	96	248,490	281,331
Coefficient of variation	0.5	0.8	1.0	1.7
Maximum	744	434	1,260,549	1,751,537
Minimum	31	14	166	269
Mean, SD of Lognormal distribution	5.3, 0.4	4.5, 0.7	12.0, 0.9	11.3, 1.2
α, β for Weibull distribution*	2.3, 249.4	1.2, 120	1.0, 237,000	0.6, 107,918
α, β for Gamma distribution*	4.7, 46.8	1.4, 81.5	1.0, 256,803	0.3, 491,083

*α = shape parameter; β = scale parameter.

4.2. Characteristics of the maximum impact pressure

Fig. 3(a) shows the measured frequency of the maximum impact pressure of the surge flow. As illustrated, the measured data are divided into 70 intervals, with a bin width of 10 kPa. In the same figure, the theoretical distributions of the four probabilistic models are also included for comparison. By comparing the measured and the theoretical frequency, Chi-square values can be calculated. Table 2 summarises the Chi-square value for each probabilistic model, the critical value at the 5% level of significance and the results of the goodness-of-fit tests.

From Table 2, the Chi-square values for the Normal, Weibull and Gamma distributions are 45, 43 and 50, respectively, which are all less than the critical value of 87 at the 5% level of significance. This suggests that the three models are acceptable for simulating the distribution of the maximum impact pressure of surge flows. On the other hand, the

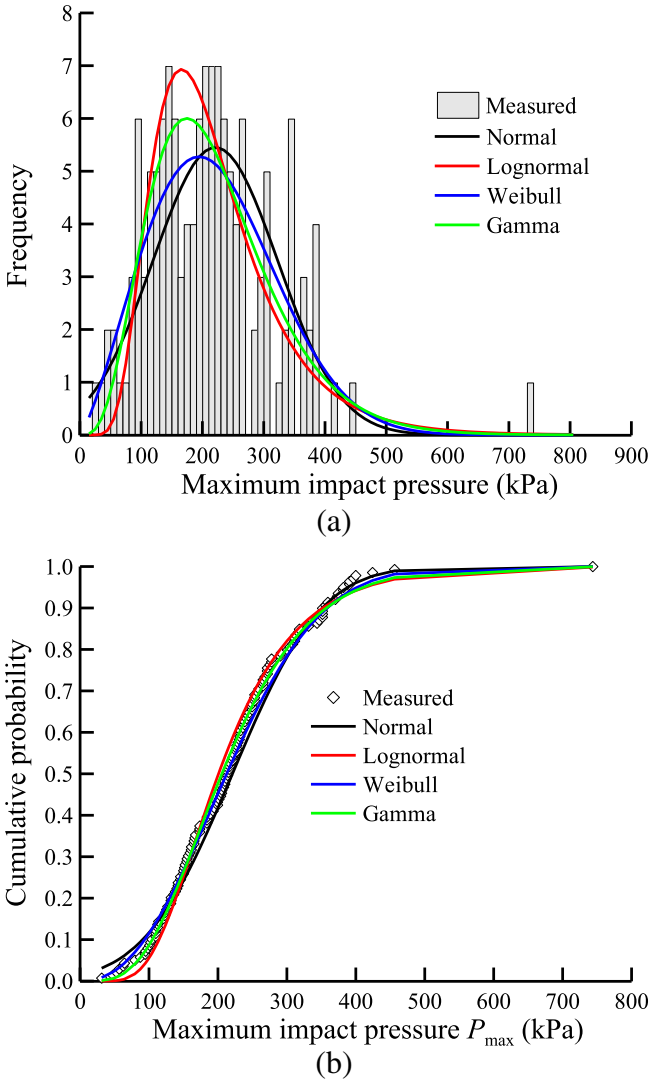

Fig. 3. Comparison of the measured and theoretically predicted (by four probabilistic models) maximum impact pressure of surge flow: (a) frequency; (b) cumulative probability.

Table 2
Results of two statistical goodness-of-fit tests for the maximum impact pressure of surge flows.

Results		Probabilistic models			
		Normal	Lognormal	Weibull	Gamma
Chi-square test	χ^2	45	140	43	50
	Rank in terms of χ^2	2	4	1	3
	Suitability	Yes	No	Yes	Yes
Kolmogorov–Smirnov test	D_n	0.06	0.07	0.05	0.05
	Rank in terms of D_n	3	4	1	1
	Suitability	Yes	Yes	Yes	Yes

Note: the critical values of the Chi-square and Kolmogorov–Smirnov tests are 87 and 0.12, respectively.

Chi-square value for the Lognormal distribution (i.e., $\chi^2 = 140$) exceeds the critical value, suggesting that this probabilistic model fails to capture the distribution of the maximum impact pressure of the surge flow. As far as the degree of goodness-of-fit is concerned, the most suitable model for simulating the maximum impact pressure is the Weibull distribution, followed by the Normal, Gamma and Lognormal distributions.

Fig. 3(b) shows the measured and the theoretical cumulative probabilities (using the four probabilistic models) of the maximum impact pressure of surge flows. Based on the measured and the calculated cumulative probability by each model, the maximum differences (D_n) between the two probabilities are calculated following the procedures of the Kolmogorov–Smirnov test. Table 2 summarises the calculated D_n values, critical values and the results of the tests. It can be seen that the D_n values for the Normal, Lognormal, Weibull and Gamma distributions are 0.06, 0.07, 0.05 and 0.05, respectively. Since these four D_n values are all smaller than the critical value (i.e., 0.12), the Kolmogorov–Smirnov test suggests that all the four probabilistic models are capable of simulating the maximum impact pressure of surge flows, at a significance level of 5%. One major difference between the two statistical goodness-of-fit tests is that the Kolmogorov–Smirnov test suggests that the Lognormal distribution is statistically suitable, while this distribution is rejected by the Chi-square test. This difference may be caused by the subjectivity (related to the artificial selection of bin size before constructing the histograms) involved in the Chi-square test, which is not included in the Kolmogorov–Smirnov test. On the other hand, both tests suggest that the Weibull distribution provides the best model simulation for the distribution of the maximum impact pressure of surge flows, while the Lognormal distribution is the least satisfactory.

Fig. 4(a) and (b) shows the measured frequency and cumulative probability of the maximum impact pressure of the continuous flows, respectively. In each figure, the theoretical distributions calculated by the four probabilistic models are also included for comparison. To examine the goodness-of-fit of the four probabilistic models to the measured distribution, Chi-square and Kolmogorov–Smirnov tests are undertaken based on the data presented in Fig. 4(a) and (b), respectively. The results of the two statistical goodness-of-fit tests for the maximum impact pressures of continuous flows are summarised in Table 3. Differing from surge flows, continuous flows can only be satisfactorily simulated by two probabilistic models, i.e., the Weibull and Gamma distributions, which have an identical level of goodness-of-fit. On the other hand, the Normal distribution is rejected by both goodness-of-fit tests.

In summary, the Weibull and Gamma distributions are found to be suitable for simulating the distributions of the maximum impact pressures of both surge and continuous flows in the Jiangjia Ravine, China.

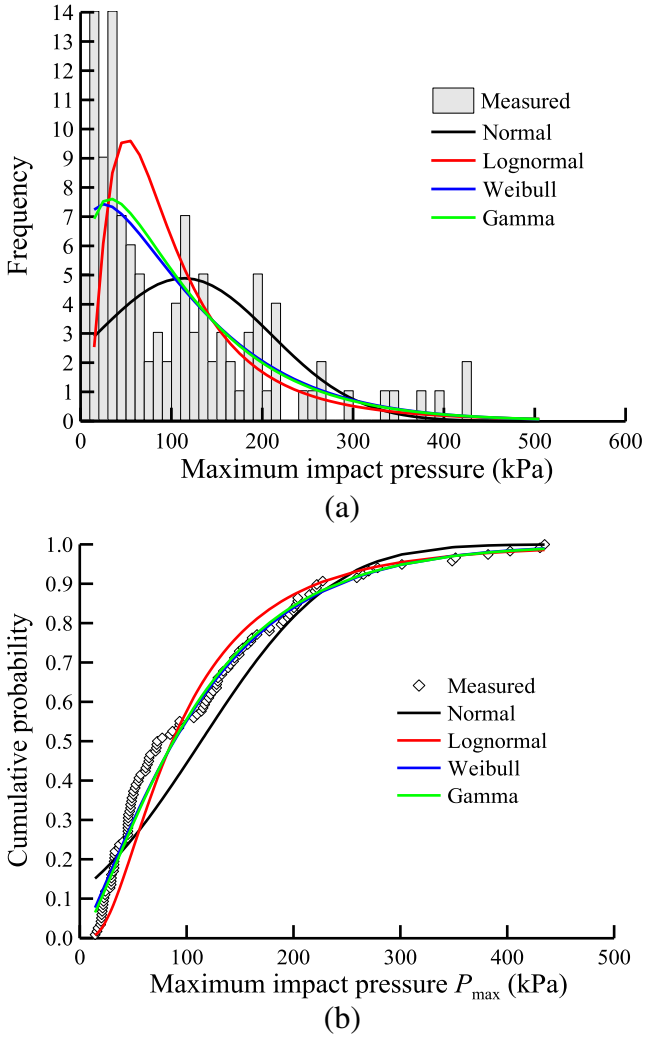

Fig. 4. Comparison of the measured and theoretically predicted (by four probabilistic models) maximum impact pressure of continuous flow: (a) frequency; (b) cumulative probability.

4.3. Characteristics of total discharge

Fig. 5(a) and (b) illustrates the frequencies and cumulative probabilities of the total discharge of surge flows, respectively. It is worth noting that in the figure, the values are based on a bin width of 8000 m^3 with 137 intervals . In each figure, the measured and theoretical (calculated by the four probabilistic models) values are compared. The degree of

Table 3
Results of two statistical goodness-of-fit tests for the maximum impact pressure of continuous flows.

Results		Probabilistic models			
		Normal	Lognormal	Weibull	Gamma
Chi-square test	χ^2	131	63	47	47
	Rank in terms of χ^2	3	2	1	1
	Suitability	No	Yes	Yes	Yes
Kolmogorov–Smirnov test	D_n	0.16	0.14	0.07	0.08
	Rank in terms of D_n	4	3	1	2
	Suitability	No	No	Yes	Yes

Note: the critical values of the Chi-square and Kolmogorov–Smirnov tests are 87 and 0.13, respectively.

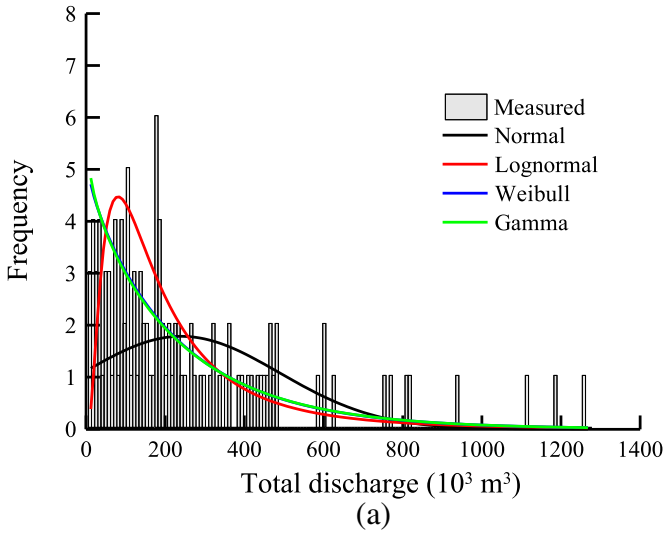

Fig. 5. Comparison of the measured and theoretically predicted (by four probabilistic models) total discharge of surge flow: (a) frequency; (b) cumulative probability.

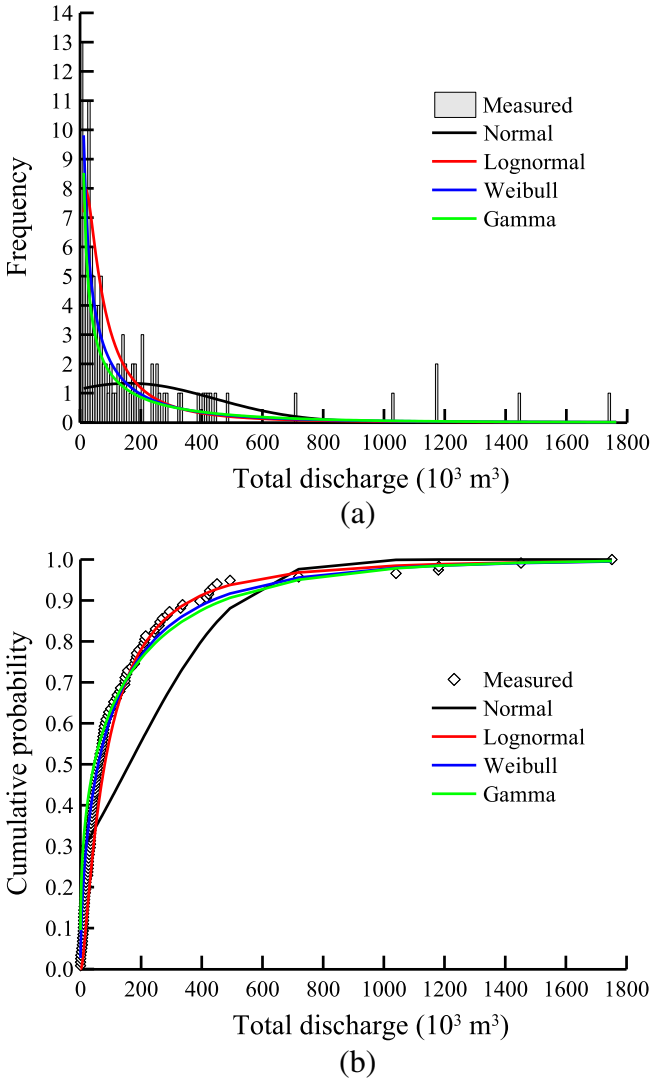

Fig. 6. Comparison of the measured and theoretically predicted (by four probabilistic models) total discharge of continuous flow: (a) frequency; (b) cumulative probability.

goodness-of-fit of each theoretical model with the measurements is evaluated by Chi-square and the Kolmogorov–Smirnov tests. Table 4 summarises the results of the two statistical goodness-of-fit tests on the four probabilistic models. According to the results of the goodness-of-fit, both tests indicate that the Weibull and Gamma distributions are acceptable among the four probability models, at a significance level of 5%. However, the Normal and Lognormal distributions fail to simulate the measured distribution of the total discharges of surge flows, from a statistical point of view.

Comparison between the measured and the theoretical frequency of the total discharge of the continuous flows is illustrated in Fig. 6(a), while the measured and the theoretical cumulative probabilities are compared in Fig. 6(b). The level of fitting between the measurements and the probabilistic models is quantified in Table 5, based on the two statistical goodness-of-fit tests. The Chi-square test suggests that the

Table 4
Results of two statistical goodness-of-fit tests for the total discharge of surge flows.

Results		Probabilistic models			
		Normal	Lognormal	Weibull	Gamma
Chi-square test	χ^2	146	135	90	90
	Rank in terms of χ^2	4	3	1	3
	Suitability	No	No	Yes	Yes
Kolmogorov–Smirnov test	D_n	0.18	0.13	0.05	0.05
	Rank in terms of D_n	4	3	1	1
	Suitability	No	No	Yes	Yes

Note: the critical values of the Chi-square and Kolmogorov–Smirnov tests are 108 and 0.12, respectively.

Table 5
Results of two statistical goodness-of-fit tests for the total discharge of continuous flows.

Results		Probabilistic models			
		Normal	Lognormal	Weibull	Gamma
Chi-square test	χ^2	445	101	91	103
	Rank in terms of χ^2	4	2	1	3
	Suitability	No	Yes	Yes	Yes
Kolmogorov–Smirnov test	D_n	0.28	0.19	0.11	0.21
	Rank in terms of D_n	4	2	1	3
	Suitability	No	No	Yes	No

Note: the critical values of the Chi-square and Kolmogorov–Smirnov tests are 108 and 0.13, respectively.

total discharge of continuous flow follows the Weibull and Gamma distributions, while the Kolmogorov–Smirnov test only considers the Weibull distribution as acceptable for simulation.

The Weibull distribution meets the minimum requirement for passing the test, i.e., with a Chi-square value almost equal to the critical value. In contrast, the other three probabilistic models are rejected by the two statistical goodness-of-fit tests.

By reviewing the aforementioned goodness-of-fit tests, it is found that the Weibull distribution is the only probabilistic model which is capable of capturing the distribution of P_{max} and Q_{total} for both surge and continuous flows, from a statistical perspective.

4.4. Correlation between the maximum impact pressure and total discharge

To explore whether there is any correlation between the maximum impact pressure and total discharge, the relationship between the two physical parameters of the surge flow is shown in Fig. 7(a). The figure is presented in a log–log scale. It can be seen that the total discharge generally increases with the maximum impact pressure. To characterise the relationship, various regression models (i.e., linear, log, exponential, power and polynomial) are attempted. Details of each regression model for surge flows are summarised in Table 6. It is found that the data can be best fitted by the following polynomial relationship:

$$\lg(Q_{total}) = -2.3^{*}\lg[(P_{max})]^2 + 12.1^{*}\lg(P_{max}) - 13.6. \quad (1)$$

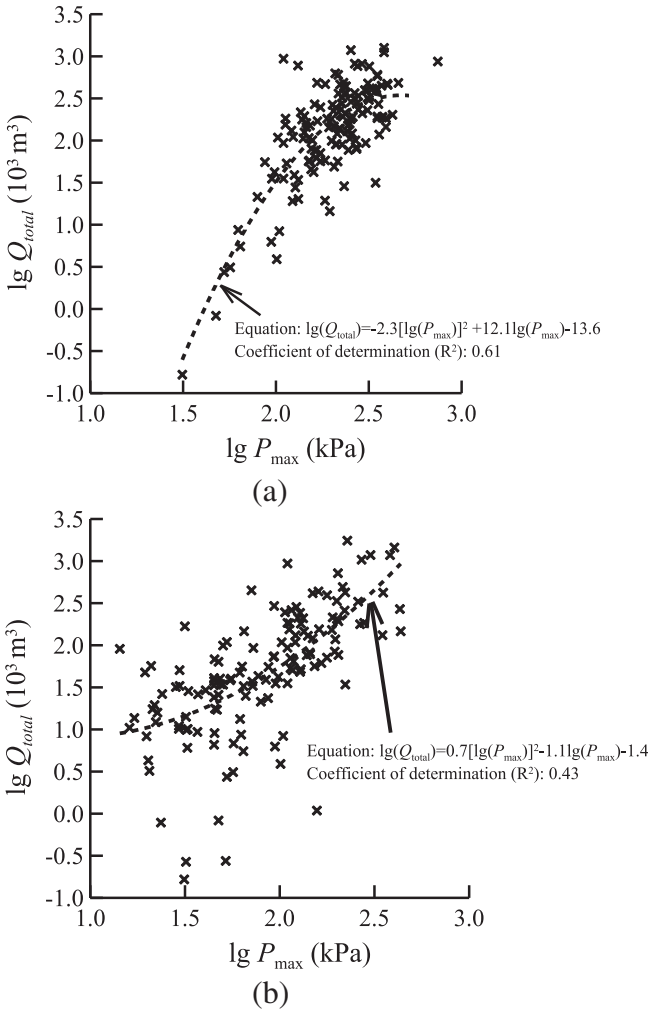

Fig. 7. Correlation between the maximum impact pressure and total discharge: (a) surge flow; (b) continuous flow.

Table 6
Details of regression models correlating P_{max} and Q_{total} of surge flows.

Regression model	Equation	Coefficient of determination (R^2)
Linear	Y = 2.1 * X − 2.7	0.54
Log	Y = 4.7 * ln(X) − 1.7	0.57
Exponential	ln(Y) = 1.1 * X − 1.9	0.46
Power	ln(Y) = 2.6 * ln(X) − 1.4	0.49
Polynomial	Y = −2.3 * X² + 12.1 * X − 13.6	0.61

Note: X and Y in the table denote log (P_{max}) and log (Q_{total}), respectively.

The coefficient of determination R^2 of the regression model is 0.61. Fig. 7(b) shows the relationship between lg(Q_{total}) and lg(P_{max}) of the continuous flow. As illustrated, the total discharge generally increases with the maximum impact pressure. By fitting the data with the commonly used regression models (i.e., linear, log, exponential, power and polynomial), it is found that the following polynomial relationship provides the best fit to the observations, as follows:

$$\lg(Q_{total}) = 0.7^{*}\lg[(P_{max})]22 - 1.1^{*}\lg[(P_{max})]2 + 1.4 \quad (2)$$

Details of other regression model for continuous flows are summarised in Table 7. The coefficient of determination of the best-fit polynomial relationship (i.e., Eq. (2)) for the continuous flow is 0.43, which is less than that (i.e., 0.61) for surge flows. This suggests that the total discharge of surge flows has a stronger correlation with the maximum impact pressure, as compared with continuous flows.

5. Exceedance probability charts for estimating the maximum impact pressure and total discharge

Considering that P_{max} and Q_{total} are two key elements in engineering design (for barriers) and risk assessment, it is worthwhile developing design charts for the two parameters, based on the analyses of this study. Since all the field data can be reasonably modelled by the Weibull distribution (as discussed in the previous section), the verified probabilistic model and model parameters can be used to develop exceedance probability design charts, as presented in the following sections.

5.1. Univariate design charts

Fig. 8(a) shows the newly developed design chart for estimating the P_{max} of both surge and continuous flows at any given exceedance probability (*EP*). It can be seen that the maximum impact pressure of the surge flows is always larger than that of the continuous flow within the full range of *EP* (i.e., 0 to 1). In addition, for an *EP* ranging from 0 to 0.3, the difference in the maximum impact pressure between surge and continuous flows increases with *EP*. These observations imply that the upper bound of the maximum impact pressure may be estimated simply based on surge flow data, if the continuous flows data are not available.

Fig. 8(b) illustrates the exceedance probability chart for Q_{total} of surge and continuous flows. Differing from P_{max} (as shown in Fig. 8(a)), the upper bound of the total discharge is not only related to

Table 7
Details of regression models correlating P_{max} and Q_{total} of continuous flows.

Regression model	Equation	Coefficient of determination (R^2)
Linear	Y = 1.4 * X − 0.9	0.42
Log	ln(Y) = 2.4 * ln(X) + 0.18	0.39
Exponential,	ln(Y) = 0.7 * X − 0.8	0.20
Power	ln(Y) = 1.2 * ln(X) − 0.3	0.19
Polynomial	Y = 0.7 * X² − 1.1 * X + 1.4	0.43

Note: X and Y in the table denote log (P_{max}) and log (Q_{total}), respectively.

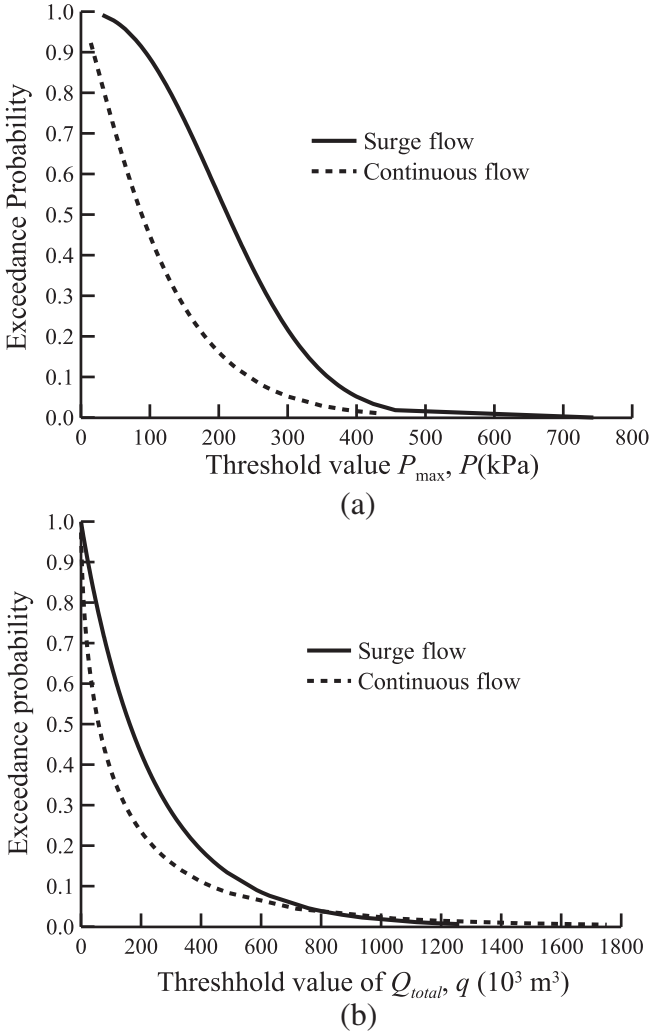

Fig. 8. Univariate exceedance probability charts for estimation of: (a) maximum impact pressure; (b) total discharge.

the flow type, but also associated with *EP*. When *EP* is relatively small (i.e., less than 0.04), Q_{total} of continuous flows is larger than that of the surge flows. The difference between the two flows reduces with *EP*. In contrast, when *EP* is larger than 0.04, Q_{total} of the continuous flow becomes smaller than that of surge flows, with the difference of Q_{total} between the two flows increasing with *EP*. These observations imply that to develop any semi-empirical design charts for total discharge, field data for both surge and continuous flows are required.

5.2. Bivariate design charts

In addition to the univariate design charts proposed in the previous section, two bivariate design charts which account for the coupling effect between P_{max} and Q_{total} are also developed for surge and continuous flows, as shown in Fig. 9. The exceedance probability in the bivariate design chart (EP_{mv}) means the occurrence probability of an event with $P_{max} > p$ or $Q_{total} > q$, i.e., $EP_{mv} = \text{Prob}[(P_{\max} > p) \cup (Q_{total} > q)]$, where p and q are threshold values of P_{max} and Q_{total}, respectively. Using De Morgan's rule (Ang and Tang, 2007), EP_{mv} can be written as

$$EP_{mv} = \text{Prob}[(P_{\max} > p) \cup (Q_{total} > q)] = 1 - \text{Prob}[(P_{\max} < p) \cap (Q_{total} < q)] \quad (3)$$

in which $\text{Prob}[(P_{\max} < p) \cap (Q_{total} > q)]$ means the occurrence probability of an event with both $P_{max} < p$ and $Q_{total} < q$, and it is given by the joint CDF of P_{max} and Q_{total}. As shown in Fig. 7, P_{max} and Q_{total} are correlated, and the Pearson correlation coefficients between them are 0.50 and 0.61 for surge and continuous flows, respectively. To incorporate the correlation between P_{max} and Q_{total} into the calculation of EP_{mv}, the Gaussian copula (e.g., Cho, 2013; Wu, 2015; Tang et al., 2013, 2015) is used to construct the joint CDF of P_{max} and Q_{total} based on their marginal distributions (see Figs. 3 to 6) and correlation coefficients. Using Gaussian copula, $\text{Prob}[(P_{\max} < p) \cap (Q_{total} > q)]$ is then written as

$$\text{Prob}[(P_{\max} < p) \cap (Q_{total} < q)] = \Phi\left\{\phi^{-1}\left[f_{P_{\max}}(p)\right]; \phi^{-1}\left[f_{Q_{total}}(q)\right]; \rho\right\} \quad (4)$$

where $\Phi\{\cdot\}$ = 2-dimensional standard Gaussian CDF; $\phi^{-1}[\cdot]$ = the inverse function of 1-dimensional standard Gaussian CDF; $f_{P_{\max}}(\cdot)$ and $f_{Q_{total}}(\cdot)$ = the respective Weibull CDFs of P_{max} and Q_{total}; ρ = correlation coefficient between the equivalent standard Gaussian random variables of P_{max} and Q_{total}, which is calculated from the correlation coefficient (e.g., 0.50 and 0.61 for surge and continuous flows, respectively) between P_{max} and Q_{total} in their original space. Details on using Gaussian copula to calculate the joint probability and construct the bivariate distribution can be referred to Wu (2015) and Tang et al. (2013, 2015).

Using Eqs. (3) and (4), the respective values of EP_{mv} for the surge and continuous flows are calculated at different threshold values, as shown in Fig. 9. Each line in the figure represents an equal-potential line of EP_{mv}. The design chart shows that the EP increases with the decreasing threshold values of P_{max} and Q_{total}. This indicates that the probability that P_{max} or Q_{total} exceeds their respective threshold values (i.e., p and q) prescribed in design increases as these prescribed values decrease. It is also shown that, for a given set of p and q values, EP_{mv} for surge flows is greater than that for continuous flows. As one of p and q is very small, EP_{mv} can always be very large regardless of the value of the other quantity. For example, as p is less than 100 kPa, EP_{mv} is always greater than 0.9 for surge flows (see Fig. 9(a)) regardless of the value of q. This is expected because EP_{mv} is dominated by the small threshold value of the maximum impact pressure, which is very likely to be exceeded. Such a design scenario should be avoided in practice.

In addition to the usefulness of the chart in engineering design, it can also provide a means to quantify the intensity of a debris flow in a probablity-based manner. For example, if a surge flow occurred with $P_{\max}$ and Q_{total} equal to 400 kPa and 800,000 m^3 (see point "A" in Fig. 9(a)), then an EP_{mv} value of 0.08 can be obtained from the chart. If the hypothesised criterion (shown in the inset to the figure) was referred to, the debris flow can be classified as "strong".

6. Summary and conclusions

To assist in engineering design and in the risk analysis of debris flows, this study presents statistical and probabilistic analyses on the maximum impact pressure and total discharge of 139 debris flow events in the "debris museum" of China (i.e., Jiangjia Ravine). Based on this study, the following conclusions can be drawn:

(a) During the period from 1961 to 2000, the maximum values of $P_{\max}$ and Q_{total} are 744 kPa and 1,751,537 m^3, respectively. The $P_{\max}$ and Q_{total} values of surge flows exhibit much larger natural variability than those of continuous flows. To be more specific, the coefficients of variation (COV) of $P_{\max}$ are 0.5 and 0.8 for surge and continuous flows, respectively, while the COVs of Q_{total} for surge and continuous flows are 1.0 and 1.7, respectively.

(b) The statistical goodness-of-fit tests show that the Weibull and Gamma distributions are the most statistically suitable for simulating P_{max} of both surge and continuous flows in

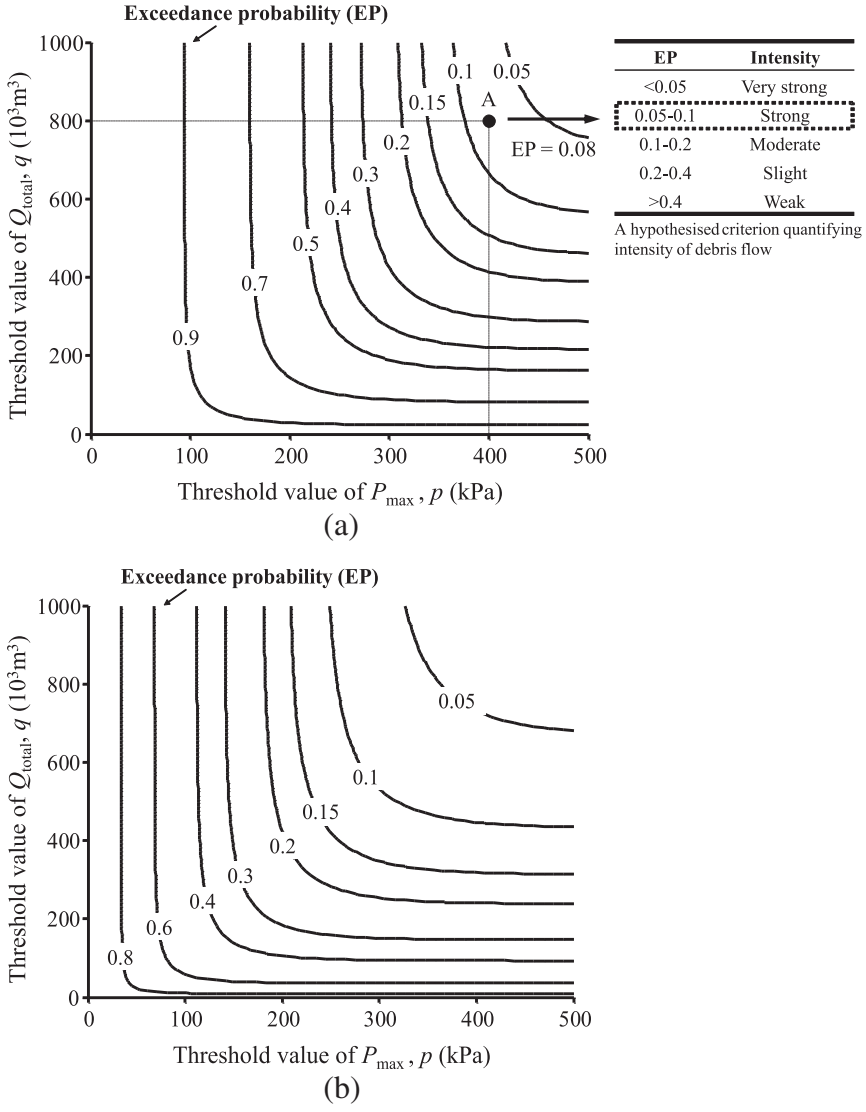

EP	Intensity
<0.05	Very strong
0.05-0.1	Strong
0.1-0.2	Moderate
0.2-0.4	Slight
>0.4	Weak

A hypothesised criterion quantifying intensity of debris flow

Fig. 9. Bivariate exceedance probability chart considering maximum impact pressure and total discharge for: (a) surge flow; (b) continuous flow.

the Jiangjia Ravine, China, among the four selected probability distributions (i.e., Normal, Lognormal, Weibull and Gamma distributions). For Q_{total} of the two flows, however, only the Weibull distribution is statistically suitable for the simulation.

(c) Based on the verified probabilistic model (i.e., Weibull) and the model parameters, exceedance probability (*EP*) charts are developed to estimate P_{max} and Q_{total} in the Jiangjia Ravine and other similar mountainous areas in Southwesten China. The design charts show that P_{max} of a surge flow is larger than that of a continuous flow at any given possibility of failure. On the other hand, Q_{total} of a continuous flow is larger than that of a surge flow at relatively small possibilities of failure ($EP < 4\%$) and the trend is reversed when *EP* is larger than 4%. In addition to the two univariate design charts, two bivariate design charts, which account for the coupling effect between P_{max} and Q_{total}, are also developed based on Gaussian copula approach.

(d) Regression models between P_{max} and Q_{total} are established by means of power laws, which are found to provide a better fit than other commonly adopted regression functions (i.e., i.e., linear, log, exponential and polynomial). The coefficients of determination (R^2) of the correlation for surge and continuous flows are 0.61 and 0.43, respectively. This suggests that Q_{total} of a surge flow has a stronger dependency on P_{max} than a continuous flow.

It is well recognised that discharge and impact pressure of a debris event strongly depend on the rainfall event. To acquire further insight into the discharge and impact pressure, it is worth correlating these two parameters with the rainfall records (such as intensity, duration and return period of rainfall) in the future.

Acknowledgements

The authors gratefully acknowledge the financial support provided by the National Science Fund for Distinguished Young Scholars of China (Project No. 51225903), the National Natural Science Foundation of China (Project No. 51409196, 51329901), the Research Grants Council of the HKSAR (Project No. HKUST6/CRF/12R) and the Hong Kong University of Science and Technology (Grants DAG12EG03S-CIVL). The valuable data collected by the Dongchuan Debris flow Observation and Research Station are also greatly appreciated.

Appendix A

Table A.1
Details of the measured data for surge flows.

Event no.	With (B): m	Thickness (h): m	Velocity (v): m/s	Density (ρ):10^3 kg / m^3	Discharge (Q_{total}): m^3	Impact pressure (P_{max}): kN / m / s^2
1	47	4.0	13	2.3	448,774	370
2	26	1.6	8	2.2	106,945	150
3	24	0.5	10	2.1	48,971	206
4	31	1.6	10	2.1	121,140	214
5	12	1.2	9	2.0	100,947	157
6	35	2.2	11	2.1	105,780	250
7	3	1.0	11	2.1	100,583	268
8	22	2.9	10	2.1	143,578	193
9	23	3.3	11	2.1	183,426	250
10	28	2.8	14	2.1	458,753	400
11	16	1.5	8	2.1	20,237	132
12	17	1.7	11	2.1	210,636	236
13	50	2.5	11	2.1	158,616	250
14	60	1.5	8	2.2	194,881	142
15	40	0.4	9	2.1	150,553	152
16	80	1.5	10	2.3	628,584	208
17	60	1.8	10	2.3	90,880	212
18	150	2.5	13	2.3	117,756	359
19	70	1.0	7	2.2	154,582	112
20	48	1.5	10	2.3	89,487	227
21	48	2.9	10	2.2	265,828	202
22	35	0.4	14	2.3	202,266	424
23	21	1.8	10	2.2	14,516	195
24	22	1.0	11	2.1	190,670	259
25	32	3.2	13	2.2	1,260,549	382
26	32	2.5	11	2.2	211,009	292
27	25	0.6	7	2.0	35,248	95
28	25	0.4	7	2.0	8385	104
29	32	2.6	13	2.3	184,462	352
30	30	2.6	13	2.3	193,073	352
31	25	0.8	7	2.0	35,364	110
32	30	2.2	12	2.3	229,272	311
33	27	1.2	10	2.2	181,121	199
34	21	1.2	10	2.2	137,559	218
35	15	1.2	10	2.2	603,269	352
36	65	3.5	13	2.3	1,117,465	382
37	60	2.5	13	2.2	768,023	275
38	45	1.8	11	2.2	76,138	161
39	35	1.6	9	2.0	387,903	308
40	55	2.1	12	2.2	179,824	253
41	50	1.7	11	2.1	413,580	331
42	50	1.3	13	2.1	166	31
43	5	0.3	4	1.8	191,511	374
44	50	1.8	13	2.3	773,10	246
45	50	1.8	11	2.2	193,37	184
46	50	0.8	9	2.2	125,162	142
47	65	1.5	8	2.1	2738	53
48	50	0.4	5	2.2	603,598	216
49	35	1.4	11	2.0	273,863	272
50	20	0.4	11	2.2	27,737	127
51	30	1.1	8	2.2	473,680	397
52	40	1.5	13	2.2	184,430	391
53	35	1.8	13	2.2	397,593	301
54	38	1.2	12	2.2	585,361	352
55	38	2.7	13	2.3	28,738	233
56	30	1.5	11	2.1	233,109	278
57	35	1.7	11	2.3	321,222	311
58	35	1.6	12	2.3	416,765	347
59	35	1.7	13	2.2	79,683	272
60	35	1.6	11	2.2	339,316	278
61	35	1.6	11	2.3	56,318	215
62	20	0.4	10	2.2	868,841	744
63	46	3.0	18	2.3	145,255	391
64	42	1.3	13	2.2	187,595	373
65	42	1.5	13	2.1	57,907	151
66	41	1.2	9	2.0	93,410	304
67	40	2.2	12	2.2	82,815	272
68	42	2.2	11	2.2	271,577	356
69	42	3.2	13	2.3	42,265	160

(continued on next page)

Table A.1 (*continued*)

Event no.	With (B): m	Thickness (h): m	Velocity (v): m/s	Density (ρ):10^3 kg / m^3	Discharge (Q_{total}): m^3	Impact pressure (P_{max}): kN / m / s^2
70	40	1.2	8	2.3	486,621	231
71	53	2.0	11	2.0	192,281	229
72	53	1.8	10	2.3	3903	101
73	40	0.5	7	2.1	58,099	184
74	53	1.5	10	2.0	477,585	313
75	53	1.3	12	2.2	151,496	244
76	52	0.8	11	2.2	276,638	227
77	54	2.5	10	2.3	367,529	239
78	54	1.8	10	2.2	45,606	155
79	60	1.0	8	2.3	147,185	205
80	60	1.2	10	2.2	99,153	199
81	58	0.8	10	2.2	56,782	174
82	60	1.0	9	2.1	128,671	241
83	61	1.8	10	2.3	777,357	131
84	64	0.8	8	2.1	110,689	124
85	20	2.0	8	2.2	89,947	210
86	20	0.5	11	1.8	362,523	217
87	45	1.8	10	2.3	42,128	98
88	35	1.0	7	2.0	169,766	167
89	40	2.5	9	2.3	216,942	136
90	35	1.5	8	2.2	5523	64
91	45	1.2	6	1.8	70,992	174
92	40	1.5	9	2.1	31,550	344
93	40	1.5	13	2.2	6282	94
94	20	0.5	7	1.9	831	48
95	4	0.5	5	1.9	483,895	456
96	30	1.5	14	2.2	53,531	114
97	25	1.2	7	2.2	303,849	317
98	35	1.5	12	2.2	139,349	221
99	22	1.0	10	2.2	106,042	140
100	25	1.1	8	2.2	181,683	189
101	20	1.2	9	2.2	21,419	79
102	13	0.8	6	2.1	55,420	87
103	16	0.6	6	2.1	108,647	102
104	15	0.6	7	2.2	316,450	265
105	18	1.2	11	2.2	3117	57
106	15	0.8	5	2.1	161,806	146
107	20	1.5	8	2.1	182,389	113
108	22	1.8	7	2.1	245,292	210
109	25	0.8	10	2.1	288,461	253
110	27	1.1	11	2.2	248,371	174
111	27	1.5	9	2.2	144,481	146
112	24	2.1	8	2.1	34,072	132
113	20	0.2	9	1.6	8689	63
114	20	0.3	6	1.8	812,654	290
115	30	1.8	12	2.1	1,185,056	253
116	20	0.9	11	2.1	269,308	161
117	30	1.7	8	2.3	441,966	238
118	35	3.6	11	2.2	225,411	204
119	35	2.4	10	2.1	93,656	110
120	27	1.0	7	2.0	177,568	138
121	25	1.7	8	2.2	468,046	184
122	22	1.1	9	2.2	438,958	232
123	28	2.8	10	2.3	485,362	166
124	26	1.4	9	2.1	131,409	121
125	15	0.4	8	2.1	77,164	165
126	23	1.7	9	2.0	80,064	155
127	28	2.5	9	2.1	56,650	150
128	25	1.8	9	2.1	464,374	222
129	25	0.5	10	2.2	936,898	110
130	20	0.6	7	2.0	62,004	165
131	25	0.7	9	2.0	356,325	233
132	40	2.5	11	2.1	365,484	265
133	42	1.6	11	2.2	234,768	224
134	43	1.3	10	2.2	38,974	126
135	20	0.3	8	2.0	818,079	265
136	50	2.1	11	2.2	757,953	318
137	53	2.8	12	2.3	322,440	227
138	45	1.3	11	2.1	121,437	257
139	35	1.2	11	2.2	19,097	123

Table A.2
Details of the measured data for continuous flows.

Event no.	With (B): m	Thickness (h): m	Velocity (v): m/s	Density (ρ):10^3 kg / m^3	Discharge (Q_{total}): m^3	Impact pressure (P_{max}): kN / m / s^2
22	20	0.6	6	1.8	25,123	66
23	6	0.2	8	2.1	78,534	145
24	25	2.7	11	2.2	177,910	265
25	25	1.3	11	2.1	184,516	279
26	22	0.3	5	1.9	38,477	55
27	4	0.2	6	1.8	6829	57
28	28	1.0	9	2.1	155,240	161
29	8	0.3	5	1.9	17,171	47
30	27	1.2	8	2.0	212,014	125
31	20	0.4	7	2.1	74,100	93
32	25	1.1	8	2.1	51,996	129
33	20	1.4	13	2.3	1,452,033	403
34	15	0.6	8	2.0	261,850	115
35	25	0.2	4	1.7	6066	33
36	50	1.0	10	2.3	193,099	204
37	20	0.4	10	2.0	84,378	195
38	15	0.3	5	1.8	40,845	45
39	50	2.0	13	2.2	131,865	348
40	40	0.5	7	1.9	38,955	85
41	50	1.5	14	2.1	146,665	435
42	5	0.3	5	1.9	25,864	48
43	40	0.4	7	2.0	23,590	87
44	30	0.4	6	2.0	37,039	72
45	10	0.3	5	1.9	40,313	48
46	5	0.3	3	1.8	10,479	16
47	10	0.3	3	1.9	17,472	21
48	20	0.5	8	2.2	129,902	141
49	18	0.5	11	2.1	1,751,537	227
50	20	0.5	6	1.9	55,991	63
51	30	1.8	11	2.3	1,180,972	301
52	10	0.5	9	2.2	393,430	178
53	30	0.6	10	2.3	76,845	204
54	20	0.7	10	2.1	214,764	190
55	20	0.5	8	1.9	50,569	117
56	30	1.2	13	2.2	1,179,609	382
57	10	0.5	8	2.2	82,139	144
58	30	0.8	7	2.1	72,875	93
59	20	0.3	5	2.0	34,522	49
60	20	0.4	5	1.9	63,813	48
61	25	0.4	8	2.0	48,441	128
62	30	0.4	6	2.1	43,227	77
63	5	0.5	8	2.1	145,836	134
64	39	0.4	5	2.1	47,527	61
65	5	0.3	5	1.8	37,664	45
66	20	0.4	5	2.0	40,153	55
67	8	0.3	7	2.1	70,496	114
68	25	0.8	13	2.3	422,075	352
69	15	0.4	4	1.9	50,723	30
70	50	0.3	10	2.0	425,248	221
71	52	1.0	9	2.3	61,526	166
72	5	0.3	3	1.7	4294	20
73	20	0.3	4	2.1	26,185	37
74	30	0.8	14	2.2	269,789	431
75	35	0.6	11	2.0	34,188	222
76	5	0.4	4	1.7	56,954	21
77	20	0.5	5	1.9	109,488	53
78	20	0.3	4	2.0	269	32
79	40	0.5	6	1.9	13,337	62
80	25	0.4	5	2.0	34,100	50
81	10	0.3	5	1.9	9070	45
82	15	0.4	4	2.1	29,251	41
83	20	0.4	5	2.0	17,706	46
84	40	1.0	6	1.8	92,955	73
85	23	0.4	4	2.0	9378	37
86	45	2.0	9	2.3	719,132	203
87	20	1.0	6	1.8	146,908	65
88	40	2.5	9	2.2	436,653	160
89	35	2.5	8	2.2	56,500	153
90	2	0.3	3	1.9	3228	21
91	14	0.3	4	1.9	785	24
92	30	0.5	9	1.9	1090	157
93	45	2.0	11	2.1	329,937	259
94	6	0.5	10	2.0	336,288	200
95	5	0.4	5	1.8	6596	45
96	20	0.3	6	2.1	32,770	64

(continued on next page)

Table A.2 (*continued*)

Event no.	With (B): m	Thickness (h): m	Velocity (v): m/s	Density (ρ):10^3 kg / m^3	Discharge (Q_{total}): m^3	Impact pressure (P_{max}): kN / m / s^2
97	25	1.2	9	2.1	152,346	188
98	20	0.5	6	2.0	32,993	72
99	12	0.3	3	2.2	26,402	24
100	12	0.5	4	1.9	32,962	30
101	13	0.4	6	2.1	450,074	71
102	9	0.4	4	2.0	14,142	32
103	15	0.4	8	2.1	108,930	121
104	15	0.6	10	2.2	259,149	220
105	20	1.0	7	2.1	293,333	93
106	16	0.7	4	1.9	31,963	28
107	15	0.8	5	2.0	99,493	50
108	25	1.0	11	2.2	1,039,867	270
109	27	2.2	10	2.2	117,917	196
110	20	0.5	5	2.0	275	52
111	10	0.5	4	1.6	168,033	32
112	10	0.3	3	1.7	90,810	14
113	10	0.2	3	1.8	8304	20
114	10	0.5	7	2.1	246,745	107
115	20	1.5	8	2.2	415,434	149
116	20	0.6	4	2.1	28,578	33
117	25	1.8	8	2.2	121,069	149
118	6	0.3	3	1.8	13,690	17
119	10	0.3	5	1.8	33,553	45
120	20	0.9	8	2.1	285,392	122
121	24	0.9	9	2.3	205,160	200
122	15	0.3	4	1.8	12,228	22
123	20	1.0	7	2.0	184,564	110
124	20	0.7	8	2.1	180,974	129
125	15	0.3	4	1.6	10,181	29
126	10	0.4	4	1.8	10,147	33
127	15	0.2	4	1.8	11,028	29
128	22	0.4	8	2.0	242,890	128
129	20	0.5	8	1.9	64,661	118
130	25	0.5	8	2.0	76,231	139
131	15	0.7	5	1.8	24,122	45
132	12	0.3	3	1.9	19,475	22
133	5	0.2	4	1.8	9887	32
134	15	0.3	3	2.1	47,639	19
135	20	1.0	10	2.2	492,871	215
136	18	0.5	5	1.9	68,217	45
137	10	0.3	3	1.9	15,867	23
138	30	1.0	10	1.9	71,448	177
139	8	0.7	8	2.1	209,794	133

References

Ang, A., Tang, W., 2007. Probability Concept in Engineering: Emphasis on Applications to Civil and Environmental Engineering. 2nd edn. John Wiley & Sons, Inc., New Jersey.

Chang, C.W., Lin, P.S., Tsai, C.L., 2011. Estimation of sediment volume of debris flow caused by extreme rainfall in Taiwan. Eng. Geol. 123, 83–90.

Cho, S.E., 2013. First-order reliability analysis of slope considering multiple failure modes. Eng. Geol. 154, 98–105.

Cui, P., Chen, X.Q., Wang, Y.Y., Hu, K.H., Li, Y., 2005. Jiang-jia Ravine debris flows in south-western China. In: Jakob, M., Hungr, O. (Eds.), Debris-flow Hazard and Related Phenomena. Springer, Berlin, pp. 565–594.

Eidsvig, U.M.K., Papathoma-Köhle, M., Du, J., Glade, T., Vangelsten, B.V., 2014. Quantification of model uncertainty in debris flow vulnerability assessment. Eng. Geol. 181, 15–26.

Fenton, G.A., Griffiths, D.V., 2008. Risk Assessment in Geotechnical Engineering. John Wiley & Sons.

Gartner, J.E., Cannon, S.H., Santi, P.M., 2014. Empirical models for predicting volumes of sediment deposited by debris flows and sediment-laden floods in the transverse ranges of southern California. Eng. Geol. 176, 45–56.

Hu, K.H., Wei, F.Q., Li, Y., 2011. Real-time measurement and preliminary analysis of debris-flow impact force at Jiangjia Ravine, China. Earth Surf. Process. Landf. 36, 1268–1278.

Iverson, R.M., 1997. The physics of debris flows. Rev. Geophys. 35 (3), 245–296.

Jiang, S.H., Li, D.Q., Zhang, L.M., Zhou, C.B., 2014a. Slope reliability analysis considering spatially variable shear strength parameters using a non-intrusive stochastic finite element method. Engineering Geology 168, 120–128.

Jiang, S.H., Li, D.Q., Cao, Z.J., Zhou, C.B., Phoon, K.K., 2014b. Efficient system reliability analysis of slope stability in spatially variable soils using Monte Carlo simulation. Journal of Geotechnical and Geoenvironmental Engineering (ASCE) http://dx.doi.org/10.1061/(ASCE)GT.1943–5606. 0001227), 04014096.

Kang, Z.C., Li, Z.F., Ma, A.N., Luo, J.T., 2004. Debris Flow Research in China. Science Press, Beijing (252 pp., in Chinese).

Kang, Z.C., Cui, P., Wei, F.Q., He, S.F., 2006. Data Collection of Observation of Debris Flows in Jiangjia Ravine, Dongchuan Debris Flow Observation and Research Station (1961–1984). Science Press, Beijing, China.

Kang, Z.C., Cui, P., Wei, F.Q., He, S.F., 2007. Data Collection of Observation of Debris Flows in Jiangjia Ravine, Dongchuan Debris Flow Observation and Research Station (1995–2000). Science Press, Beijing, China.

Ngadisih, Yatabe R., Bhandary, N.P., Dahal, R.K., 2014. Integration of statistical and heuristic approaches for landslide risk analysis: a case of volcanic mountains in West Java Province. Indonesia. Georisk 8 (1), 29–47.

Li, D.Q., Qi, X.H., Zhou, C.B., Phoon, K.K., 2014. Effect of spatially variable shear strength parameters with linearly increasing mean trend on reliability of infinite slopes. Structural Safety 49, 45–55.

Li, J., Yuan, J.M., 1983. The main features of the mudflow in Jiang-Jia Ravine. Z. Geomorphol. N.F. 27 (3), 325–341.

Liang, W., Zhuang, D., Jiang, D., Pan, J., Ren, H., 2012. Assessment of debris flow hazards using a Bayesian Network. Geomorphology 171–172, 94–100.

Tang, X.S., Li, D.Q., Zhou, C.B., Phoon, K.K., 2015. Copula-based approaches for evaluating slope reliability under incomplete probability information. Struct. Saf. http://dx.doi.org/10.1016/j.strusafe.2014.09.007.

Tang, X.S., Li, D.Q., Rong, G., Phoon, K.K., Zhou, C.B., 2013. Impact of copula selection on geotechnical reliability under incomplete probability information. Computers and Geotechnics 49, 264–278.

Wang, J.P., Chan, C.H., Wu, Y.M., 2011. The distribution of annual maximum earthquake magnitude around Taiwan and its application in the estimation of catastrophic earthquake recurrence probability. Nat. Hazards 59, 553–570.

Wang, Y., Cao, Z., 2013. Probabilistic characterization of Young's modulus of soil using equivalent samples. Engineering Geology 159, 106–118.

Wang, J.P., Huang, D.R., Chang, S.C., Wu, Y.M., 2014. New evidence and perspective to the Poisson process and earthquake temporal distribution from 55,000 events around Taiwan since 1900. Nat. Hazards Rev. 15 (1), 38–47.

Wu, X.Z., 2015. Assessing the correlated performance functions of an engineering system via probabilistic analysis. Struct. Saf. 52, 10–19.

Zhang, S., 1993. A comprehensive approach to the observation and prevention of debris flows in China. Nat. Hazards 7, 1–23.

Zhang, J., Xiong, G., 1997. Data Collection of Kinematic Observation of Debris Flows in Jiangjia Ravine, Dongchuan, Yunnan (1987–1994). Science Press, Beijing, China.

Zhou, G.G.D., Ng, C.W.W., 2010. Dimensional analysis of natural debris flows. Can. Geotech. J. 47 (7), 719–729.